Supporting Information

Two-dimensional Janus XWZAZ' (X=S, Se, Te; A=Si, Ge; Z, Z'=N, P, As)：Candidates for Photocatalytic Water Splitting and Piezoelectric Materials

Zhen Gao[a], Hongbo Wu[b,c], YaoHe[a,]*, and Kai Xiong[d,]*

[a]*Department of Physics, Yunnan University, Kunming 650091, People's Republic of China.*

[b]*School of Science, Yangzhou Polytechnic Institute, Yangzhou 225127, China.*

[c]*College of Physics, Hebei Normal University, Shijiazhuang 050024, People's Republic of China*

[d]*Materials Genome Institute, School of Materials and Energy, Yunnan University, Kunming 650091, P. R. China.*

*E-mail:
yhe@ynu.edu.cn；xiongkai@ynu.edu.cn

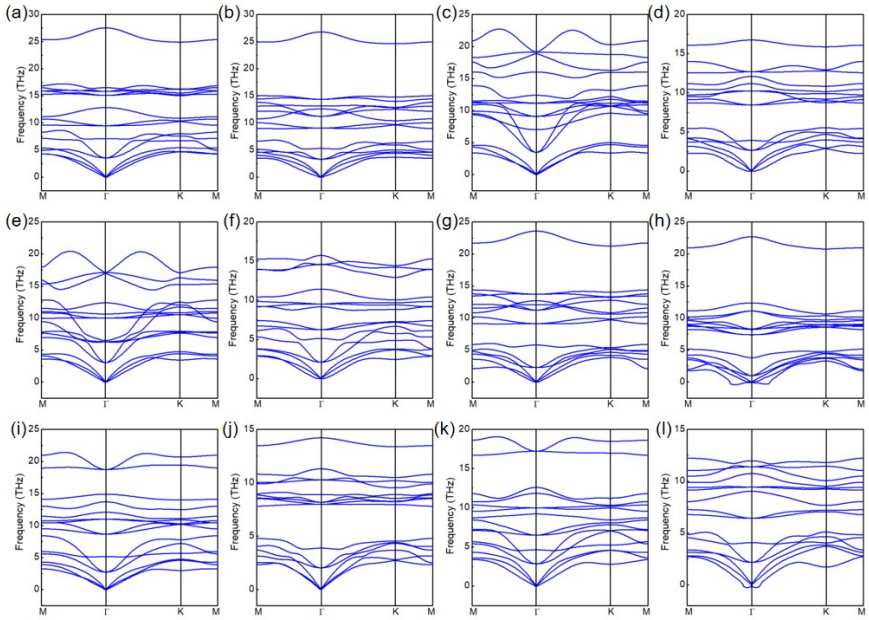

Fig S1 Phonon dispersions of the (a)SWNSiP, (b)SWNSiAs, (c) SWPSiN, (d) SWPSiAs, (e) SWAsSiN, (f) SWAsSiP, (g) SWNGeP, (h)SWNGeAs, (i) SWPGeN, (j) SWPGeAs, (k) SWAsGeN, and (l) SWAsGeP layers, respectively.

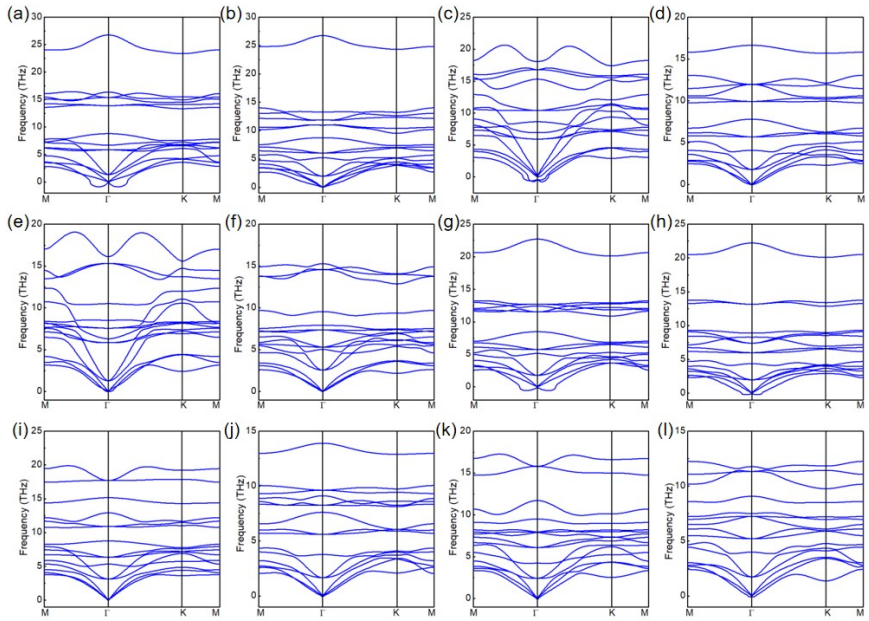

Fig S2Phonon dispersions of the (a)SeWNSiP, (b)SeWNSiAs, (c) SeWPSiN, (d) SeWPSiAs, (e) SeWAsSiN, (f) SeWAsSiP, (g) SeWNGeP, (h)SeWNGeAs, (i) SeWPGeN, (j) SeWPGeAs, (k) SeWAsGeN, and (l) SeWAsGeP layers, respectively.

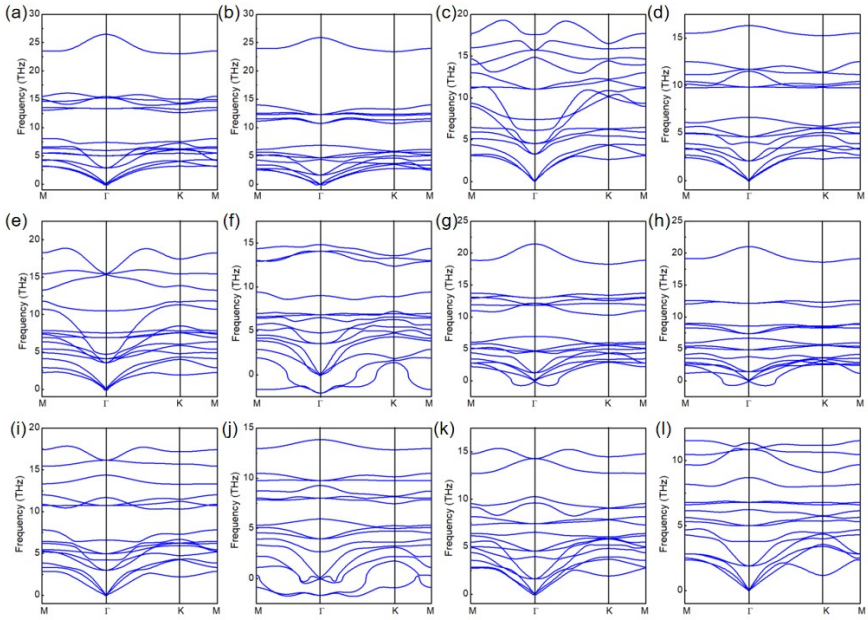

Fig S3 Phonon dispersions of the (a)TeWNSiP, (b)TeWNSiAs, (c) TeWPSiN, (d) TeWPSiAs, (e) TeWAsSiN, (f) TeWAsSiP, (g) TeWNGeP, (h)TeWNGeAs, (i) TeWPGeN, (j) TeWPGeAs, (k) TeWAsGeN, and (l) TeWAsGeP layers, respectively.

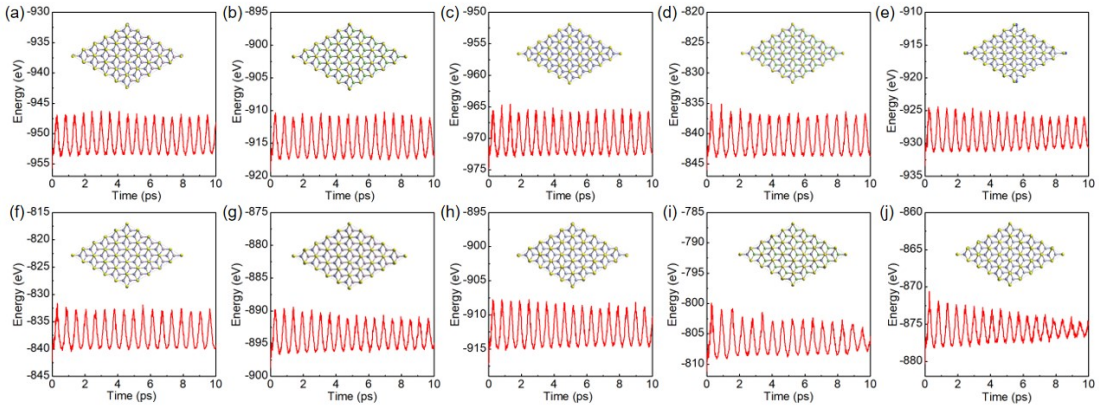

Fig S4Variation of the energy as a function of time for the Janus (a) SWNSiP, (b) SWNSiAs, (c) SWPSiN, (d) SWPSiAs, (e) SWAsSiN; (f) SWAsSiP; (g) SWNGeP, (h) SWPGeN, (i) SWPGeAs, and (j) SWAsGeN layers at 300K. The insets are the top views of the structure at the end of the AIMD simulation.

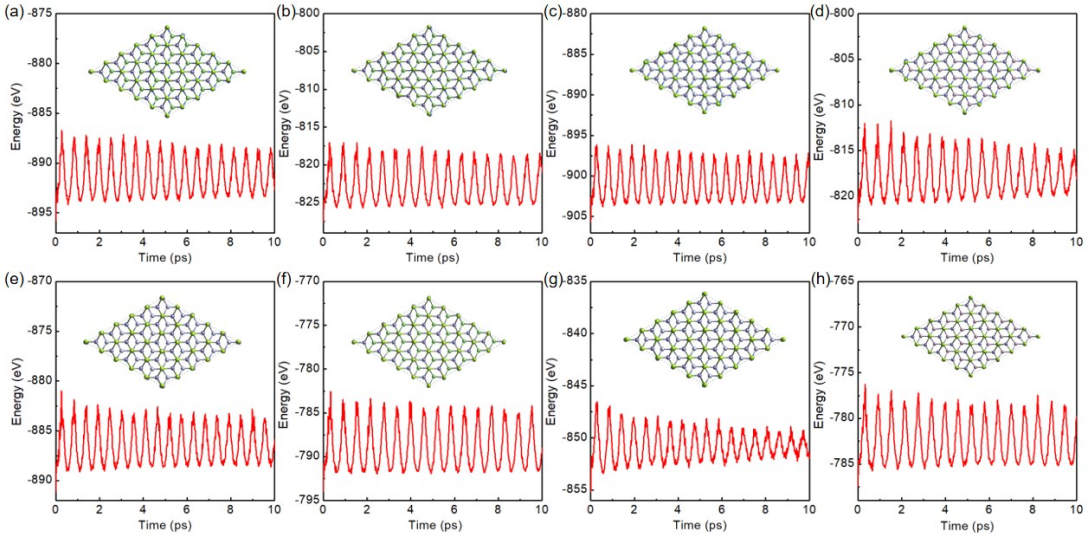

Fig S5 Variation of the energy as a function of time for the Janus (a) SeWNSiAs, (b) SeWPSiAs, (c) SeWAsSiN, (d) SeWAsSiP, (e) SeWPGeN; (f) SeWPGeAs; (g) SeWAsGeN, and (h) SeWAsGeP layers at 300K. The insets are the top views of the structure at the end of the AIMD simulation.

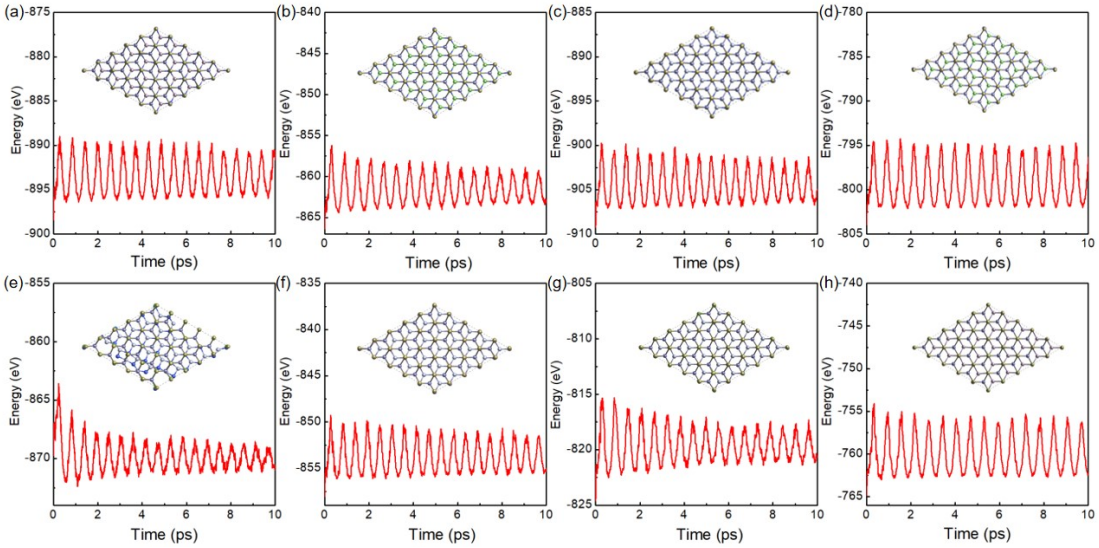

Fig S6Variation of the energy as a function of time for the Janus (a) TeWNSiP, (b) TeWNSiAs, (c) TeWPSiN, (d) TeWPSiAs, (e) TeWAsSiN; (f) TeWPGeN; (g) TeWAsGeN, and (h) TeWAsGeP layers at 300K. The insets are the top views of the structure at the end of the AIMD simulation.

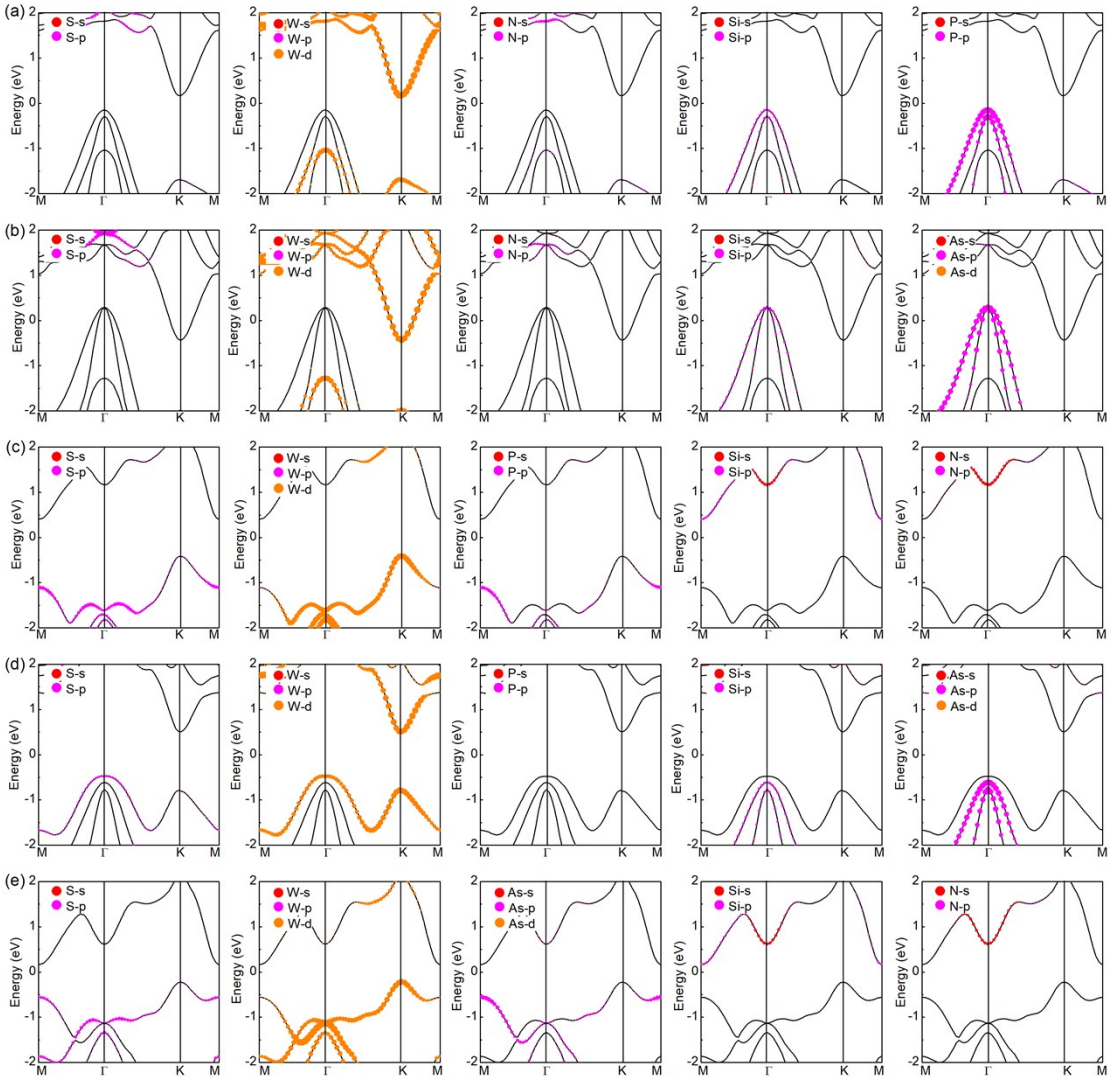

Fig S7Projected band structure of 2D Janus(a) SWNSiP, (b) SWNSiAs, (c) SWPSiN, (d) SWPSiAs, (e) SWAsSiN layers at equilibrium.

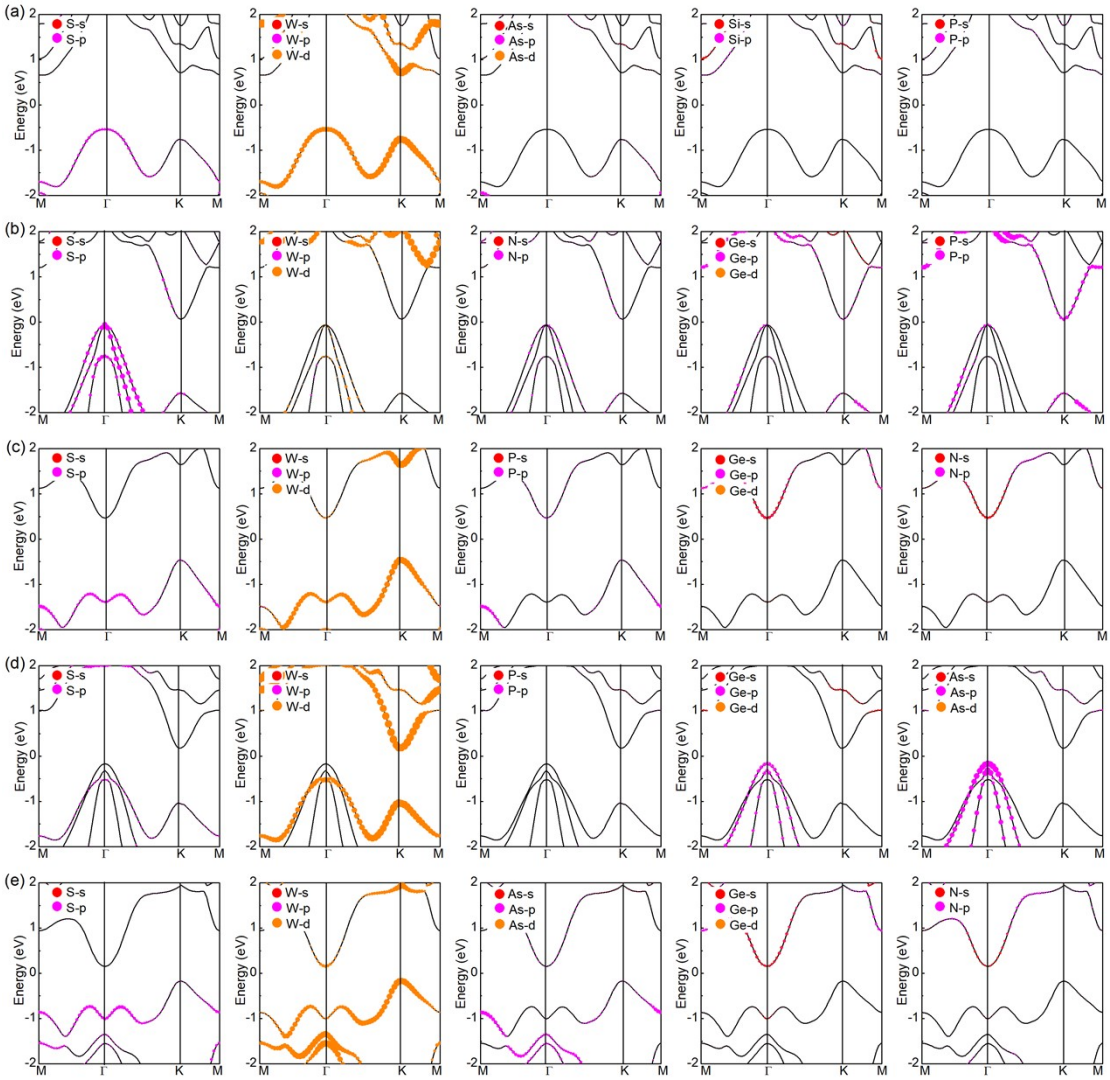

Fig S8 Projected band structure of 2D Janus(a) SWAsSiP, (b) SWNGeP, (c) SWPGeN, (d) SWPGeAs, and (e) SWAsGeN layers at equilibrium.

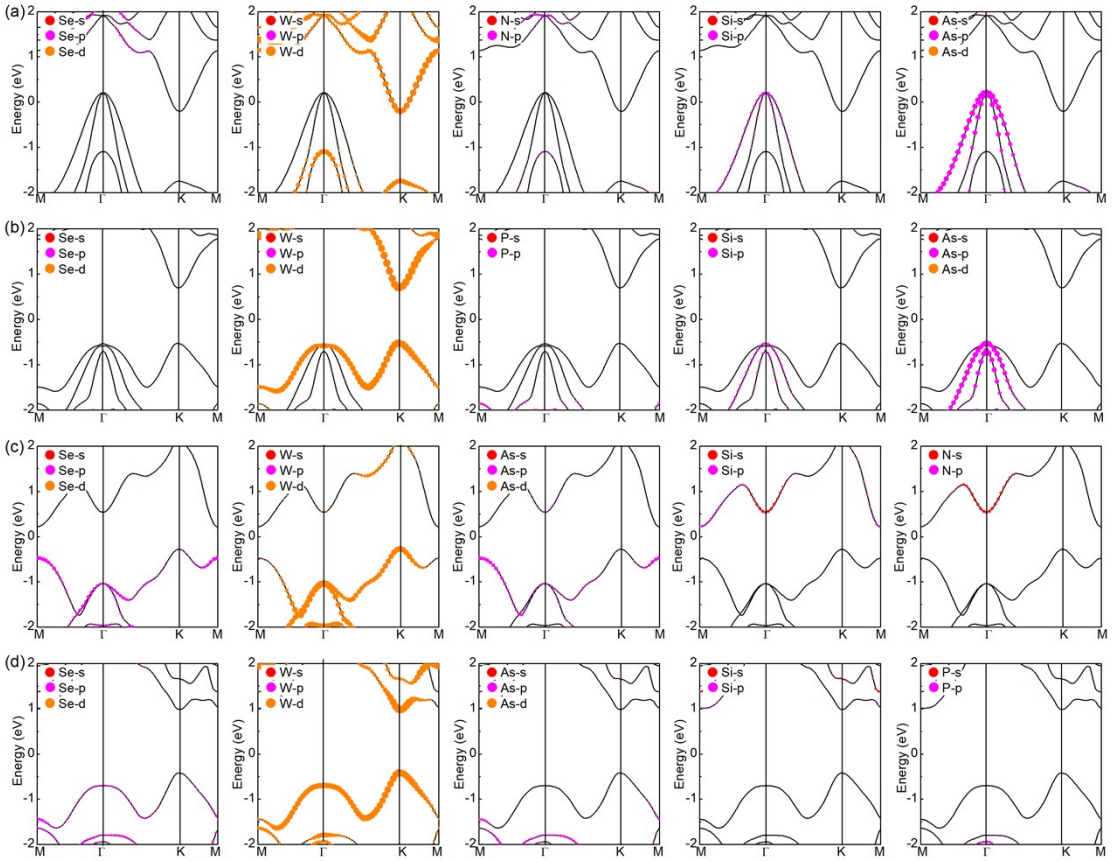

Fig S9Projected band structure of 2D Janus(a) SeWNSiAs, (b) SeWPSiAs, (c) SeWAsSiN, and (d) SeWAsSiP layers at equilibrium.

Fig S10Projected band structure of 2D Janus(a) SeWPGeN, (b) SeWPGeAs; (c) SeWAsGeN, and (d) SeWAsGeP layers at equilibrium.

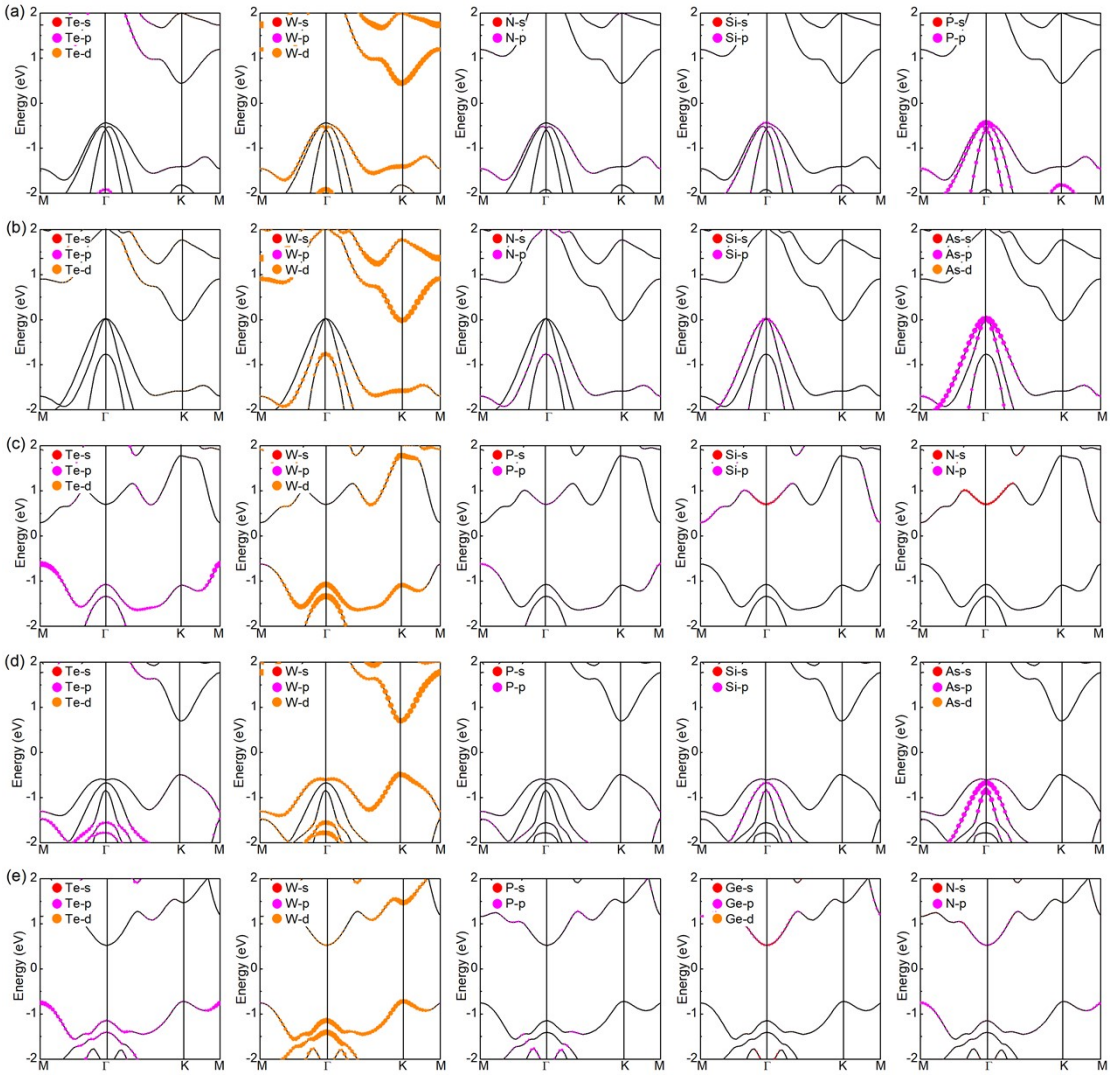

Fig S11Projected band structure of 2D Janus(a) TeWNSiP, (b) TeWNSiAs, (c)TeWPSiN, (d) TeWPSiAs, and (e) TeWPGeN layers at equilibrium.

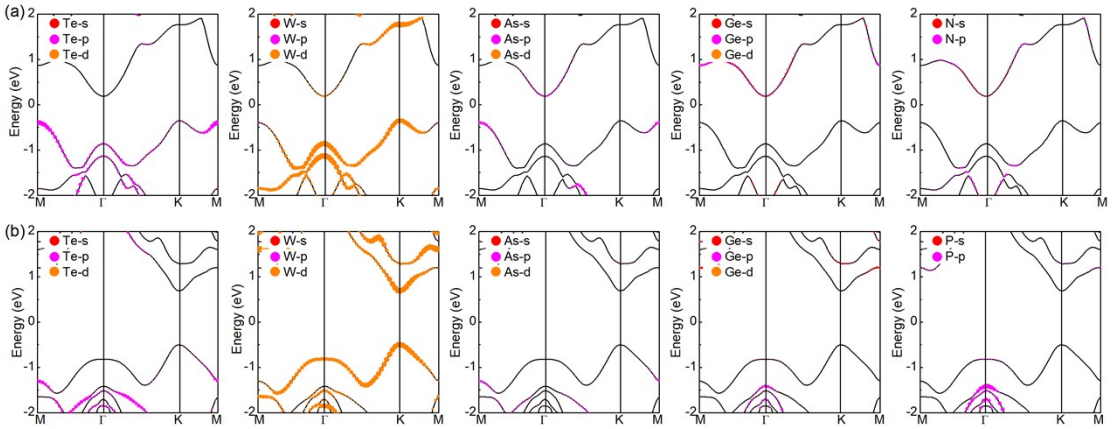

Fig S12 Projected band structure of 2D Janus(a) TeWAsGeN, and (b) TeWAsGeP layers at equilibrium.

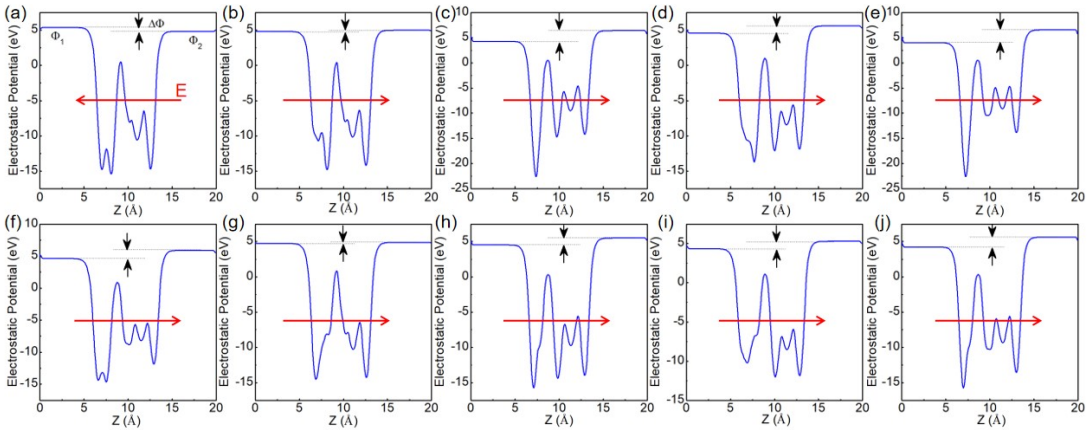

Fig S13Electrostatic potential of 2D Janus(a) SWNSiP, (b) SWNSiAs, (c) SWPSiN, (d) SWPSiAs, (e) SWAsSiN, (f) SWAsSiP, (g) SWNGeP, (h) SWPGeN, (i) SWPGeAs, and (j) SWAsGeN layers.

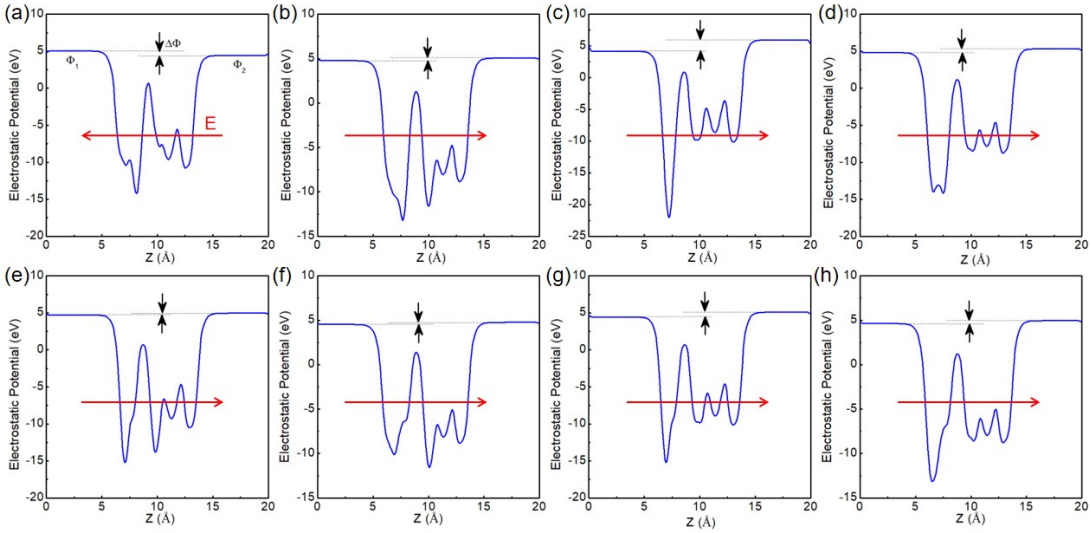

Fig S14Electrostatic potential of 2D Janus(a) SeWNSiAs, (b) SeWPSiAs, (c) SeWAsSiN, (d) SeWAsSiP, (e) SeWPGeN, (f) SeWPGeAs, (g) SeWAsGeN, and (h) SeWAsGeP layers.

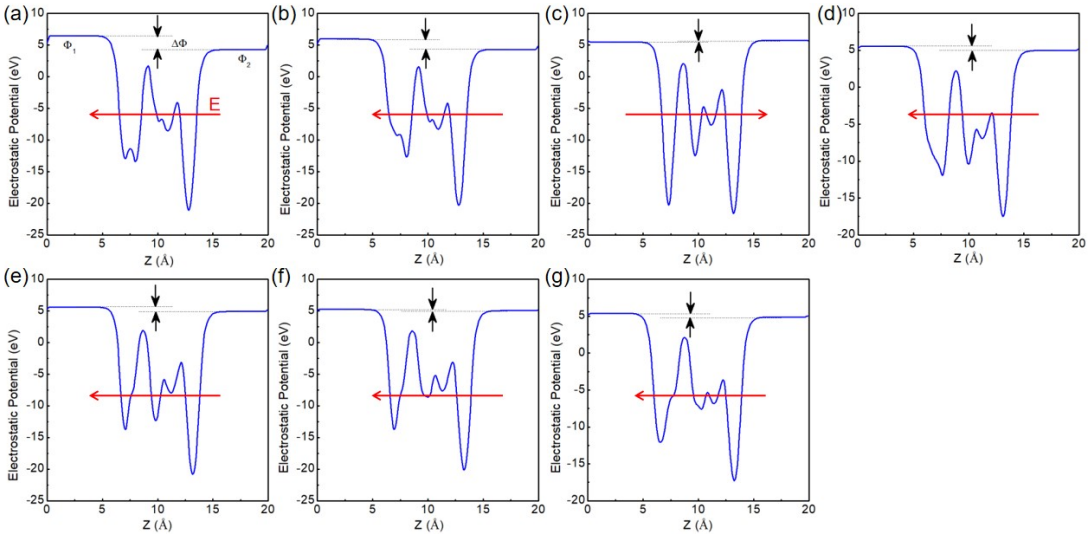

Fig S15Electrostatic potential of 2D Janus(a) TeWNSiP, (b) TeWNSiAs, (c)TeWPSiN, (d) TeWPSiAs, (e) TeWPGeN, (f) TeWAsGeN, and (g) TeWAsGeP layers.

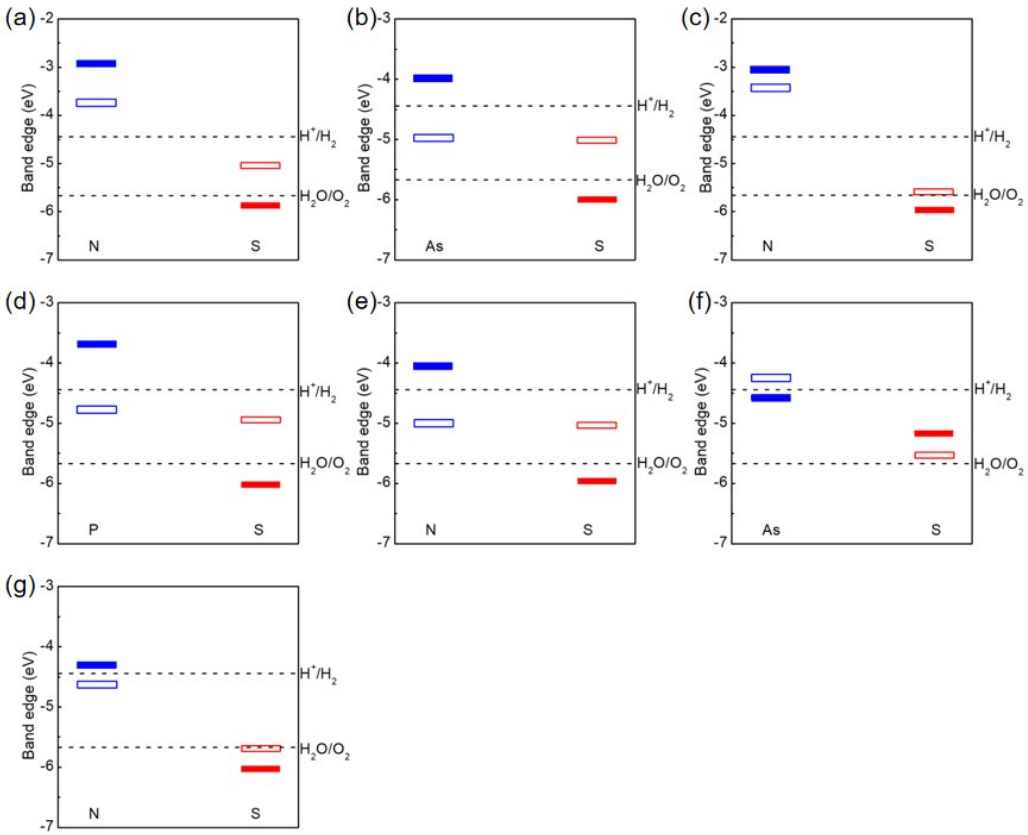

Fig S16 The band edges with respect to the redox potential of water for (a)SWPSiN, (b) SWPSiAs, (c) SWAsSiN, (d) SWAsSiP, (e) SWPGeN, (f) SWPGeAsand (g) SWAsGeN layers. The hollow rectangle indicates the absence of CBM and VBM, and only the solid rectangles are physically meaningful.

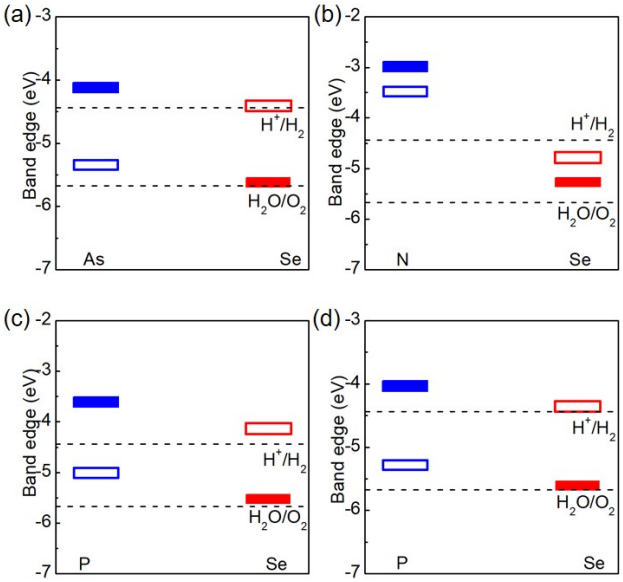

Fig S17The band edges with respect to the redox potential of water for (a)SeWPSiAs, (b) SeWAsSiN, (c) SeWAsSiP, and (d) SWAsGeP layers. The hollow rectangle indicates the absence of CBM and VBM, and only the solid rectangles are physically meaningful.

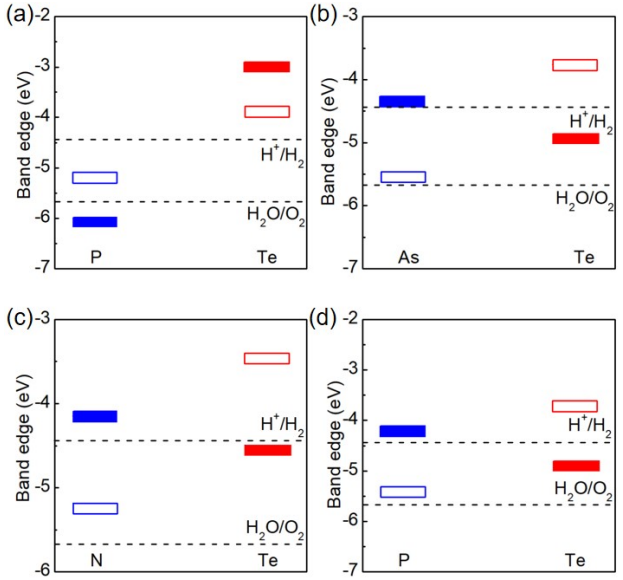

Fig S18The band edges with respect to the redox potential of water for (a)TeWNSiP, (b) TeWPSiAs, (c)TeWPGeN, and (d) TeWAsGeP layers. The hollow rectangle indicates the absence of CBM and VBM, and only the solid rectangles are physically meaningful.

The Solar-to-hydrogen (STH) Efficiency

The STH efficiency is evaluated using the methods proposed by Yang et al.[1]According to the reaction process, STH efficiency is defined as the product of the efficiency of light absorption (η_{abs}) and carrier utilization (η_{cu}).

$$\eta_{STH} = \eta_{abs} \times \eta_{cu} \tag{S1}$$

The efficiency of light absorption is defined as:

$$\eta_{abs} = \frac{\int_{E_g}^{\infty} P(h\omega)d(h\omega)}{\int_{0}^{\infty} P(h\omega)d(h\omega)} \tag{S2}$$

where $P(h\omega)$ are the AM1.5G solar energy flux at the photon energy $h\omega$ and E_g is the band gap of the materials. The denominator represents the total power density of the reference sunlight spectrum (AM1.5G) and the numerator gives the light power density absorbed by the photocatalyst.

The efficiency of carrier utilization (η_{cu}) is defined as:

$$\eta_{cu} = \frac{\Delta G_{H_2O} \int_{E}^{\infty} \frac{P(h\omega)}{h\omega} d(h\omega)}{\int_{E_g}^{\infty} P(h\omega)d(h\omega)} \tag{S3}$$

where ΔG_{H_2O} is the free energy of water splitting (1.23eV) and the rest of numerator represents the effective photocurrent density. Here, E represents the photon energy that can be actually utilized in the process of water splitting.

$$E = \begin{cases} E_g, \left(\chi(H_2) \geq 0.2, \chi(O_2) \geq 0.6\right) \\ E_g + 0.2 - \chi(H_2), \left(\chi(H_2) < 0.2, \chi(O_2) \geq 0.6\right) \\ E_g + 0.6 - \chi(O_2), \left(\chi(H_2) \geq 0.2, \chi(O_2) < 0.6\right) \\ E_g + 0.8 - \chi(H_2) - \chi(O_2), \left(\chi(H_2) < 0.2, \chi(O_2) < 0.6\right) \end{cases} \tag{S4}$$

The intrinsic electric field does positive work for the electron-hole separation during the process of photocatalytic water splitting. Therefore, this part of work should be added into the total energy, and then the corrected STH efficiency of photocatalytic water splitting for 2D material with vertical intrinsic E_F is calculated as:

$$\eta_{STH}^{'} = \eta_{STH} \times \frac{\int_0^{\infty} P(h\omega)d(h\omega)}{\int_0^{\infty} P(h\omega)d(h\omega) + \Delta V \int_{E_g}^{\infty} \frac{P(h\omega)}{h\omega} d(h\omega)} \quad \text{(S5)}$$

where ΔV is the vacuum level difference on the two respective surfaces.

Free Energy Difference (ΔG)

Free energy difference (ΔG) in the water redox reactions is calculated according the approach proposed by Nørskov*et al.*[2]The formula at pH=0 without solar irradiation can be defined as below:

$$\Delta G = \Delta E + \Delta E_{zpe} - T\Delta S \quad \text{(S6)}$$

where ΔE is the adsorption energy, ΔE_{zpe} and ΔS are the difference in zero point energy and entropy difference between the adsorbed state and the gas phase, respectively.

There are four steps to transform H_2O into O_2 molecule in oxidation half reaction, which can be written as:

$$* + H_2O \rightarrow OH^* + H^+ + e^- \quad \text{(S7)}$$

$$OH^* \rightarrow O^* + H^+ + e^- \quad \text{(S8)}$$

$$O^* + H_2O \rightarrow OOH^* + H^+ + e^- \quad \text{(S9)}$$

Meanwhile, hydrogen production half reaction can be decomposed into two steps, the reaction equation can be written as:

$$* + H^+ + e^- \rightarrow H^* \quad \text{(S10)}$$

$$H^* + H^+ + e^- \rightarrow * + H_2 \quad \text{(S11)}$$

where * means the adsorbed materials, O^*, OH^*, OOH^* and H^* represent the adsorbed intermediates.

For each reaction of both oxidation and hydrogen production, the free energy difference under the effect of pH and extra potential bias can be written as:

$$\Delta G_a = G_{OH*} + \frac{1}{2}G_{H_2} - G_* - G_{H_2O} + \Delta G_U - \Delta G_{pH} \quad \text{(S12)}$$

$$\Delta G_b = G_{O*} + \frac{1}{2}G_{H_2} - G_{OH*} + \Delta G_U - \Delta G_{pH} \quad \text{(S13)}$$

$$\Delta G_c = G_{OOH*} + \frac{1}{2}G_{H_2} - G_{O*} - G_{H_2O} + \Delta G_U - \Delta G_{pH} \quad \text{(S14)}$$

$$\Delta G_d = G_* + \frac{1}{2}G_{H_2} + G_{O_2} - G_{OOH*} + \Delta G_U - \Delta G_{pH} \quad \text{(S15)}$$

$$\Delta G_e = G_{H*} - \frac{1}{2}G_{H_2} - G_* + \Delta G_U + \Delta G_{pH} \quad \text{(S16)}$$

$$\Delta G_f = G_* + \frac{1}{2}G_{H_2} - G_{H*} + \Delta G_U + \Delta G_{pH} \quad \text{(S17)}$$

where ΔG_{pH} ($\Delta G_{pH} = k_B T \times ln10 \times pH$) represents the free energy contributed in different pH concentration. ΔG_U ($\Delta G_U = -eU$) denotes extra potential bias provided by an electron in the electrode, where U is the electrode potential relative to the standard hydrogen electrode (SHE).

Table S1 Zero-point energy correction (E_{ZPE}), and entropy contribution (TS, T=298.15K) of molecules and adsorbates.

Species	ZPE	-TS
H_2	0.27	-0.41
H_2O	0.56	-0.67
OH*	0.299	-0.093
O*	0.080	-0.055
OOH*	0.403	-0.196

(1) Fu, C.-F.; Sun, J.; Luo, Q.; Li, X.; Hu, W.; Yang, J. Intrinsic Electric Fields in Two-dimensional Materials Boost the Solar-to-Hydrogen Efficiency for Photocatalytic Water Splitting. *Nano Lett.* **2018**, *18*, 6312-6317.

(2) Nørskov, J. K.; Rossmeisl, J.; Logadottir, A.; Lindqvist, L.; Kitchin, J. R.; Bligaard, T.; Jónsson, H. Origin of the Overpotential for Oxygen Reduction at a Fuel-Cell Cathode. *J. Phys. Chem. B* **2004**, *108*, 17886-17892.